Journal of Environmental Management 395 (2025) 127767

Contents lists available at ScienceDirect

Journal of Environmental Management

journal homepage: www.elsevier.com/locate/jenvman

Research article

# Detected or not? Remote sensing measurements from the latest Euro 6d vehicles across Europe.

Zhuoqian Yang [a], Christopher Rushton [b], James Tate [b,*]

[a] School of Transportation and Logistics, Southwest Jiaotong University, Chengdu, 611756, China
[b] Institute for Transport Studies, University of Leeds, Leeds, LS2 9JT, UK

ARTICLE INFO

Handling Editor: Lixiao Zhang

*Keywords:*
Limit of detection
Emission monitoring
Remote sensing
Diesel vehicles
High-emitter identification

ABSTRACT

Incorporating real-driving emission tests into type approval procedures has significantly reduced emissions from diesel passenger cars. Recent remote sensing studies suggest that $NO_x$ emissions from the latest Euro 6d series (including both Euro 6d-TEMP and Euro 6d) are extremely low, in some cases approaching zero. This study investigates whether these low $NO_x$ concentrations fall below the detection limits of remote sensing devices, potentially limiting the reliability of measured values. A method is proposed to estimate the limit of detection using electric vehicle measurements, which serve as low-emission references in the absence of calibration gases. $NO_x$ data from six recent European remote sensing campaigns (2021–2023) were analyzed. The findings suggest that $NO_x$ emissions from the latest Euro 6d series vehicles that are in good working order have reached the detection limit of OPUS RSD 5000 devices. This approach presents a practical framework for routinely determining the detection limits of remote sensing devices, improving quality assurance procedures and supporting the interpretation of ultra-low $NO_x$ emission measurements with greater confidence.

## 1. Introduction

Nitrogen Oxides ($NO_x$) emissions from diesel vehicles significantly contribute to urban air pollution globally (Carslaw et al., 2011; Smit et al., 2022; Yang et al., 2024). For pre-Euro 6 diesel cars, substantial discrepancies have been reported between laboratory type-approval tests and real-world on-road measurements (Chen and Borken-Kleefeld, 2014). Since the introduction of Euro 6ab in 2014, the $NO_x$ limit for diesel passenger cars has been reduced by 55 % compared with Euro 5, leading to a substantial reduction in on-road emissions (Söderena et al., 2020; Yang et al., 2022). With Euro 6d-TEMP and Euro 6d, real-driving emission (RDE) tests became mandatory, ensuring that aftertreatment systems such as selective catalytic reduction (SCR) operate effectively under real-world conditions (García-Contreras et al., 2021). Consequently, on-road measurements confirm that Euro 6d-TEMP and Euro 6d diesel cars comply with the EU $NO_x$ emission limits (Suarez-Bertoa et al., 2019; de Ruiter et al., 2020; Mulholland et al., 2022).

Remote sensing technology, as a key emission monitoring method for analyzing the real-world emission performance of vehicle fleets is indicating that both the mean and median $NO_x$ emissions from the latest Euro 6d vehicles are very low (Mahesh et al., 2023; Bernard et al., 2023). This finding raises a critical question: are current remote sensing devices (RSDs) accurately capturing the emission concentrations from low-emitting Euro 6 cars, or are the results merely reflecting the detection limits of the devices?

This study compiles 359,502 valid remote-sensing measurements of European passenger cars from six campaigns conducted between 2021 and 2023 under the CARES,[1] ReMOVES[2] and CONOX projects (Borken-Kleefeld et al., 2018). The first objective is to quantify real-world $NO_x$ emissions across Euro standards, with emphasis on the latest Euro 6d-TEMP and Euro 6d diesel vehicles and whether their observed levels are genuinely near zero across Europe, which would bring them in line with Euro 5 and 6 gasoline vehicles with their Three-Way Catalytic (TWC) converters that are known to effectively control $NO_x$ emissions (Carslaw et al., 2011). To interpret these ultra-low readings, an assessment of instrument detectability is then undertaken. Using the growing sample of electric-drive vehicles as low-concentration references, a Laplace fit is used to characterize background noise and derive campaign-specific limits of detection for

* Corresponding author.
*E-mail address:* J.E.Tate@its.leeds.ac.uk (J. Tate).
[1] https://cares-project.eu/.
[2] https://www.aramis.admin.ch/Texte/?ProjectID=45536.

https://doi.org/10.1016/j.jenvman.2025.127767
Received 5 August 2025; Received in revised form 15 October 2025; Accepted 22 October 2025
Available online 27 October 2025

the remote sensing instruments. These LoD estimates are then used to contextualise the Euro-class emission distributions and to distinguish signal from noise.

There are three key contributions to the existing literature. First, it proposes a practical method for estimating the limit of detection (LoD) of remote sensing devices under field conditions, where calibration gas blending facilities are not available. This method offers a straightforward approach for data analysts to determine whether a $NO_x$ measurement falls below the device's detection limit at that time. Second, by applying this method to a cross-campaign remote sensing database (Rushton et al., 2025), the study reveals that a substantial proportion of $NO_x$ measurements from the latest Euro 6d-TEMP and Euro 6d diesel passenger cars fall below the estimated detection limits of current remote sensing systems, indicating a fundamental shift in the detectability of $NO_x$ emissions from modern diesel vehicles using current remote sensing technology. Third, the empirical evidence on the practical limits of current remote sensing technologies provides valuable technical insights for future campaign design, instrument development, and policy implementation. These findings are considered very timely as the European Commission plans to introduce large-scale remote sensing under its upcoming 'Roadworthiness Package' (European Commission, 2025). This includes proposing wide-scale, routine use of vehicle emission remote sensing to screen at least 30 % of its registered fleet in all 27 EU member states to improve detection of defective vehicles, subsequent roadside inspection and remedial action.

## 2. Literature review

### 2.1. Remote sensing technology principles and applications

Remote sensing technology has become an important and cost-effective method for monitoring real-world vehicle emissions at the fleet level (Huang et al., 2018). These systems estimate exhaust emissions rapidly and non-intrusively under actual driving conditions by measuring the absorption of specific wavelengths of light by gas molecules (Bishop and Stedman, 1996). Pollutant concentrations are typically expressed as ratios to $CO_2$ and can be converted to fuel-specific (g/kg) or distance-specific (g/km) emission factors (ICCT, 2018; Davison et al., 2020).

RSDs also collect vehicle speed, acceleration, license plate data, and environmental conditions (e.g., temperature, pressure, humidity) during measurements, enabling large-scale fleet sampling without disrupting traffic (Grange et al., 2019; Yang et al., 2022). Their results are widely used to evaluate emission trends across standards, identify high-emitting vehicles or manufacturers, and assess the influence of driving conditions on emissions (Chen et al., 2020; Huang et al., 2019; Yang et al., 2022).

Emissions from the latest Euro 6d diesel light-duty vehicles are significantly lower than their Euro 5 predecessors, raising concerns that the reliability of remote sensing measurement results is decreasing, with the recorded values becoming closer to the background noise level rather than reflecting the true pollutant concentration. For example, Knoll et al. (2024) observed that EDAR systems consistently underestimated $NO_2$ emissions compared to Portable Emissions Measurement Systems (PEMS). They attributed this discrepancy to the possibility that primary nitrogen dioxide ($NO_2$) emissions are already below the detection limit of the EDAR devices.

### 2.2. Background noise and limit of detection

When remote sensing devices measure vehicle emissions, even if the target pollutant (such as $NO_x$) is entirely absent, the devices themselves still record minor random fluctuations or interference signals, manifested as measured values randomly fluctuating around zero (Gruening et al., 2019; Yang et al., 2022). Sources of background noise include: (1) inherent random fluctuations from the instrument's electronic components and detectors; (2) interference caused by environmental conditions (e.g., temperature fluctuations, humidity changes, or ambient particulates); (3) residual plumes from earlier traffic on the same or from traffic of nearby lanes (Huang et al., 2018; Smit et al., 2021). In this study, we focus specifically on quantifying the background noise originating from the instrument itself, rather than broader atmospheric or traffic-related variability, as the former determines the intrinsic detection capability of the remote sensing system.

If the actual pollutant concentration is extremely low, the recorded values are indistinguishable from a blank measurement. Therefore, acknowledging and quantifying background noise and instrument offsets is essential for accurate interpretation of remote sensing data during emission measurement campaigns. In remote sensing emission studies, background noise is typically quantified as the standard deviation of measurements obtained using blank samples or test samples with concentrations of analyte close to or below the expected LoD (Cantwell, 2025). For instance, using certified calibration gas cylinders, Ropkins et al. (2017) determined the background noise of the EDAR device[3] to be 7 ppm for NO, while Rushton et al. (2018) reported a background noise level of 58 ppm for NO for the RSD 4600 instrument.[4]

When certified gas cylinders of different concentrations (or blends) are not available, some studies interpret the negative values recorded by RSDs as manifestations of background noise. Pokharel et al. (2001) identified the Laplace distribution as the most appropriate model for characterizing this noise pattern. In subsequent work, Bishop and Stedman (2014) used the Laplace distribution and reported a background noise level of 30 ppm for NO from the FEAT system.[5]

Since the ability of an instrument to detect a pollutant depends on how clearly the signal stands out from the background noise, the concept of the LoD is often used to define the lowest concentration that can be reliably distinguished from background noise (Crowther, 2001; Armbruster and Pry, 2008). LOD are normally calculated by multiplying a standard deviation (i.e., background noise) by a suitable factor. U.S. Environmental Protection Agency (2015) and Cantwell (2025) estimate the LoD as three times the standard deviation. Thus, accurately identifying and quantifying background noise is fundamental to determining the LoD of remote sensing instruments and evaluating the reliability of remote sensing monitoring data.

In conclusion, although several studies have acknowledged the presence of instrument noise in remote sensing, few have systematically examined its specific characteristics or the corresponding limits of detection, particularly for newer devices. Given that $NO_x$ emissions from the latest Euro 6d vehicles are extremely low, understanding the detection limits of current remote sensing instruments has become increasingly important for ensuring accurate interpretation of measurement results.

## 3. Materials and methods

### 3.1. Remote sensing instrumentation and measurement setup

The remote sensing measurements analyzed in this paper were measured by two different commercial instruments (the OPUS RSD (Carslaw and Rhys-Tyler, 2013) and the HEAT EDAR (Ropkins et al., 2017)), both providing measurements of Nitric Oxide (NO) and Nitrogen dioxide ($NO_2$). The OPUS RSD is a cross-road remote sensing system that combines non-dispersive infrared (NDIR) for CO, $CO_2$, and HC detection with non-dispersive dispersive ultraviolet (NDUV) spectroscopy for NO and $NO_2$ (see Fig. 1-a). (Bishop and Stedman, 1996). Specifically, NO is measured at 227 nm and $NO_2$ at 438 nm. By measuring the amount of IR/UV light absorbed and subtracting the pre-vehicle background

[3] https://www.heatremotesensing.com/edar.
[4] https://opusrse.com/technology/the-remote-sensing-device/.
[5] https://digitalcommons.du.edu/feat/.

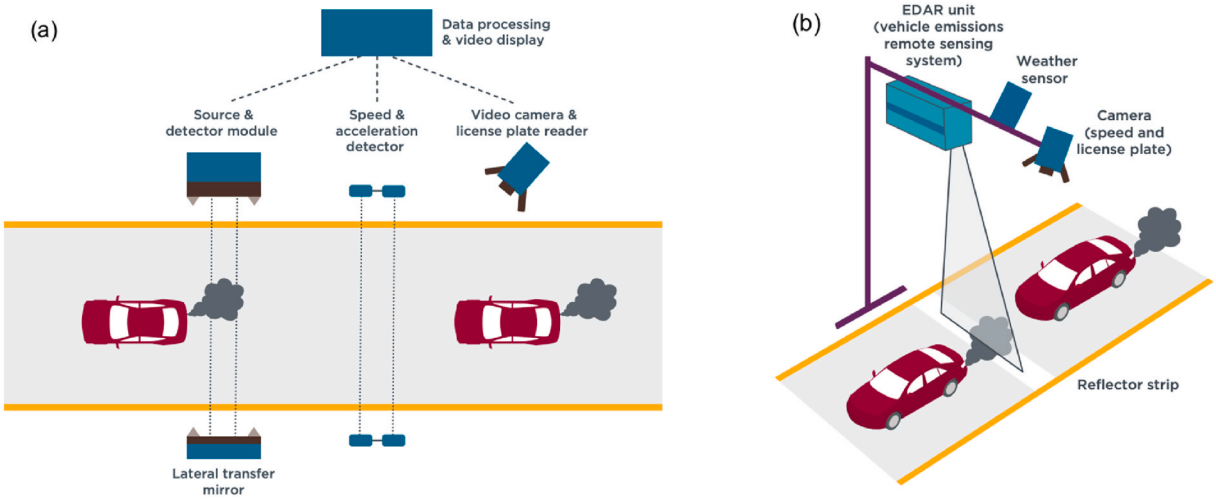


**Fig. 1.** Schematics of a typical remote sensing deployment: (a) cross-road remote sensing system [left]; (b) top-down remote sensing system (EDAR) [right] (Borken-Kleefeld and Dallmann, 2018).

absorption, the pollutant levels in the exhaust plume can be determined. The HEAT EDAR is a top-down remote sensing system using a laser-based DIAL (Differential Absorption LiDAR) method (see Fig. 1-b). It determines gas concentrations by emitting two laser beams at different wavelengths (one at the gas absorption peak and one outside it) and comparing the differences in their backscattered signals to quantify the gas absorption (Weitkamp, 2005).

While OPUS RSD uses NDIR and NDUV method and HEAT EDAR uses DIAL method, both systems fundamentally operate on the principle of detecting specific wavelengths of light absorbed by gas molecules to determine gas concentrations remotely and non-intrusively. This commonality ensures that both systems can effectively monitor and measure gas emissions in various settings. The ReMOVES project in Switzerland in 2021 used both the HEAT EDAR and OPUS RSD instruments and found that these two instruments provided comparable $NO_x$ values for both diesel and petrol passenger cars (Betschart et al., 2022), therefore in this paper it is considered appropriate to be able to directly compare results measured by the OPUS RSD and the HEAT EDAR instruments.

### 3.2. Sample description

#### 3.2.1. Measurement sites and campaigns

From 2021 to 2023, several measurement campaigns were conducted across Europe, primarily under the auspices of three major initiatives: the H2020-funded CARES project, the ReMOVES project, and the CONOX project. A detailed description is provided below in Table 1. The ReMOVES project selected 8 suitable sites in Switzerland in 2021, and both the HEAT EDAR and the OPUS RSD were used in these campaigns. In the CARES project, three measurement campaigns were carried out in cities across Europe (i.e., Milan, Krakow, and Prague). The emission records were captured by the HEAT EDAR instruments in Milan while the other cities used the OPUS RSD instruments. The latest dataset is from the CONOX project, carried out in Switzerland in 2023 using the OPUS RSD devices.

#### 3.2.2. Fuel type and emission standard

Fig. 2 illustrates the sample size collected during each campaign and the proportion of different fuel types. Campaigns were dominated by either diesel or petrol vehicles, with the remaining share consisting of hybrid electric vehicles (HEVs), battery electric vehicles (BEVs), and vehicles powered by liquefied petroleum gas (LPG). The campaign in Krakow had the most records, with approximately 113,300 valid measurements from passenger cars. In most campaigns, petrol-powered cars dominated the share of measurements (on average 51.0 %), with diesel cars being slightly less common (on average 37.8 %). In Prague, the situation was the opposite, with diesel-powered cars being the dominant

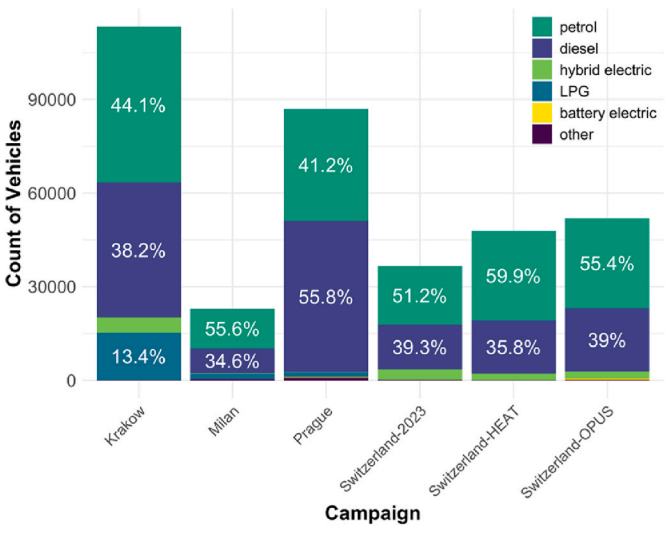


**Fig. 2.** Distribution of vehicle fuel type for passenger cars in each campaign.

**Table 1**
Campaign description.

| Project | Site information | Campaign code | Year | Dates | Device | Sample size |
|---|---|---|---|---|---|---|
| CARES | Poland - Krakow | Krakow | 2021 | Nov 30 - Dec10 | OPUS | 113,306 |
| CARES | Italy - Milan | Milan | 2021 | Sept 23 - Oct 8 | HEAT | 22,959 |
| CARES | Czech Republic - Prague | Prague | 2022 | Sept 5 - Sept 23 | OPUS | 86,890 |
| ReMOVES | Switzerland - 3 sites | Switzerland - HEAT | 2021 | May 29 - Jun 11 | HEAT | 47,886 |
| ReMOVES | Switzerland - 8 sites | Switzerland - OPUS | 2021 | Apr 26 - Jun 17 | OPUS | 51,895 |
| CONOX | Switzerland - Zurich | Switzerland-2023 | 2023 | NA | OPUS | 36,566 |

type (55.8 %). Fig. 2 also illustrates the share of HEVs and BEVs on road. BEVs were nearly absent in most campaigns, with only 0.3 % recorded in Prague and 0.7 % in Switzerland-OPUS. Similarly, HEVs remained a minority fuel type, with the highest share observed in the Switzerland-2023 campaign at 9.1 %, followed by Krakow, Switzerland-HEAT, and Switzerland-OPUS, each in the 4 % range. In Milan, hybrids accounted for less than 1 % of the fleet and were entirely absent in the Prague dataset.

The detailed information on emission standard of diesel passenger cars in each campaign is identified by cross-referencing recorded number plates with vehicle registration records. The Euro standard composition for diesel passenger cars is illustrated in Fig. 3. For most of the campaigns, the dominant emission standards are Euro 5 and Euro 6a/b/c, with one exception: Euro 4 cars in Krakow still account for 27.2 % of the total vehicles. Prague has the highest percentage of the latest Euro 6d passenger cars comprising 9.0 %, even higher than the campaign carried out one year later in Switzerland in 2023 (7.7 %).

### 3.2.3. Driving conditions

As ambient temperature (Grange et al., 2019), road grade and engine load (expressed as Vehicle Specific Power) (Gallus et al., 2017) all have an impact on the emission performance of the vehicles, it is necessary to study and account for the driving conditions in each campaign (with brief summaries provided in Table 2 and detailed distribution plots presented in Table S. 1 in the Supplementary materials). Among these factors, ambient temperature can also affect instrument noise through its influence on detector stability and optical response. In contrast, road grade and engine load primarily affect the plume shape and signal strength rather than the background noise. Additionally, remnant exhaust plumes from preceding vehicles may interfere with background light intensity measurements, thereby contributing to apparent noise in the recorded data.

Ambient temperature varied across different campaigns: the three campaigns in Switzerland and the campaign in Milan all had a median temperature around 22 °C, while the campaign in Prague had a lower median temperature of 15 °C. Krakow had the lowest median ambient temperature of 5.7 °C as the campaign was carried out in the winter months. High $NO_x$ emissions from diesel cars are expected in Krakow, as low temperatures are not conducive to the optimal efficiency of $NO_x$ emission control systems (e.g. EGR and SCR) commonly deployed on diesel engines (Smit et al., 2025). Road grade at all RSD sites was positive, as guidance (Borken-Kleefeld, 2013) recommends deploying on a slightly uphill slop to increase likelihood engines are under load. The

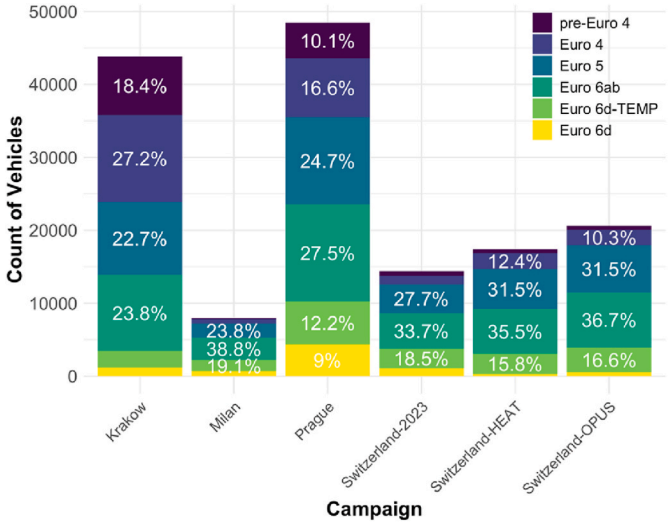


**Fig. 3.** Composition of emission standard of diesel passenger cars in each campaign.

**Table 2**
Median ambient temperature, road grade, speed, acceleration and VSP values of different campaigns.

| Campaign | Ambient temperature (°C) | Road grade (%) | Speed (km/h) | Acceleration (km/h/s) | VSP (kW/ton) |
|---|---|---|---|---|---|
| Krakow | 5.7 | 1.2 | 40.0 | 1.3 | 9.4 |
| Milan | 22.0 | 0.1 | 30.4 | 0.3 | 3.7 |
| Prague | 14.7 | 1.4 | 31.2 | 2.2 | 10.4 |
| Switzerland-HEAT | 22.0 | 0.7 | 95.4 | 0.6 | 18.2 |
| Switzerland-OPUS | 25.6 | 1.6 | 35.0 | 0.3 | 6.4 |
| Switzerland-2023 | 25.7 | NA | 49.3 | 0.4 | 13.9 |

speed and acceleration data illustrates that the vehicles captured by the RSDs have a typical speed between 30 km/h and 60 km/h, while the acceleration is mainly between 1 km/h/s and 2 km/h/s. The Vehicle Specific Power (VSP) values in the last column are calculated based on vehicles instantaneous speed/acceleration, road grade and vehicle type (Jiménez-Palacios, 1999). VSP values provide a metric of the instantaneous load on the engine to overcome rolling resistance, aerodynamic drag, acceleration and hill climbing per unit of mass of the vehicle; and are closely correlated with fuel consumption and tail-pipe emission levels. The 2021 campaign in Switzerland, which used the EDAR HEAT device, took place in a highway setting (multiple lanes). This environment had higher average speeds of around 90 km/h and VSP values of approximately 18.2 kW/ton. In contrast, the Milan campaign that took place on slower urban roads had a median VSP value of about 3.7 kW/ton.

### 3.3. Fitting distributions to fleet emissions

Fleet-level emissions are often summarized using the mean. However, numerous studies (Bishop et al., 2012; ICCT, 2018; Chen et al., 2019) have shown that $NO_x$ emissions from diesel vehicles typically exhibit right-skewed distributions, where a small proportion of high-emitting vehicles can substantially increase the mean value. Fig. 4 illustrates this pattern using data from the Switzerland–OPUS campaign. In symmetrical distributions, the mean, median, and mode are approximately equal, whereas in right-skewed distributions, a few high-emitting vehicles can significantly influence the mean, making it less representative of the fleet's overall behavior. The mode, defined as the peak of the fitted probability density function, provides a more practical measure of the most common or "typical" emission level within a fleet.

Based on the observed right-skewed and symmetrical patterns of emission distributions, the Gumbel and Laplace distributions were selected for fitting. The Gumbel distribution was chosen for the right-skewed data; this choice is supported by previous studies (Pokharel et al., 2001; Rushton et al., 2021; Yang et al., 2022) and is particularly suitable as it can accommodate the small negative values arising from measurement noise. For the more symmetrical distributions, the Laplace model was selected over the conventional normal distribution because our instrument noise data exhibited sharper peaks and heavier tails than a normal bell shape. This choice is justified by consistently higher $R^2$ values from comparative fits and is consistent with prior remote sensing studies (Pokharel et al., 2001).

For each vehicle group, the $NO_x$ emission data were fitted to both distributions by maximum likelihood estimation (MLE). The goodness of fit was evaluated using the coefficient of determination ($R^2$) and Anderson–Darling test, and the distribution with the higher $R^2$ (and higher Anderson–Darling test p-value) was selected. Approximate 95 % confidence intervals for the fitted parameters were obtained via nonparametric bootstrapping (1000 replicates). The mode of the best-

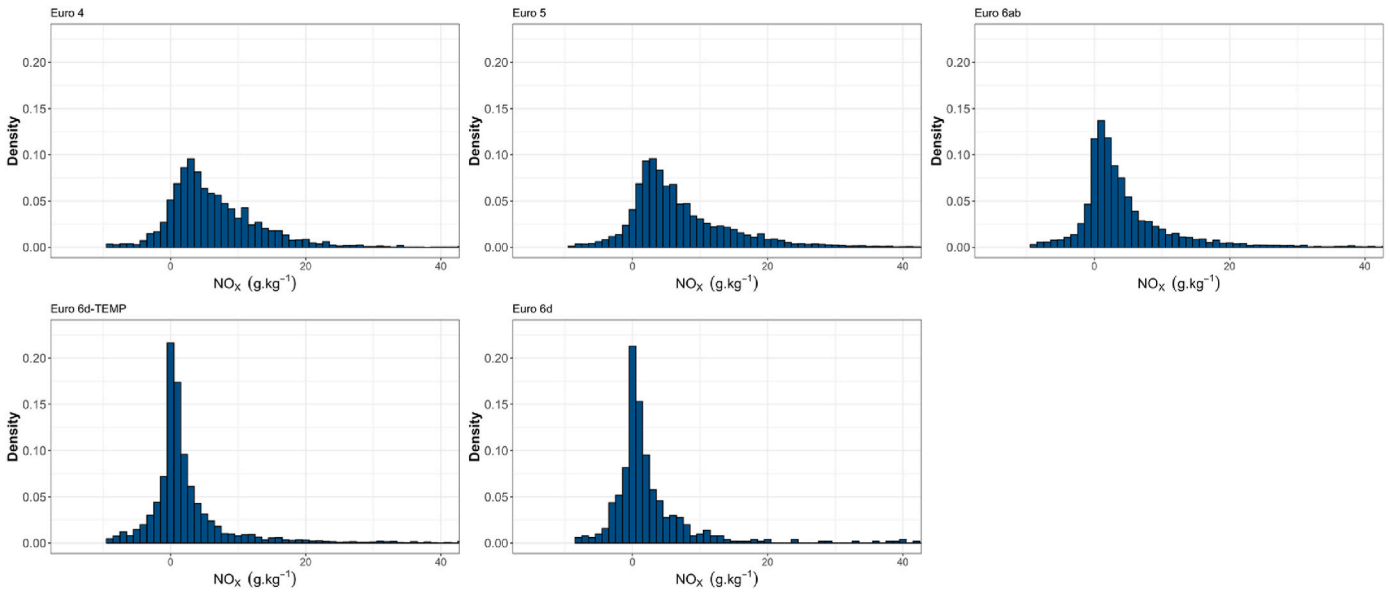


**Fig. 4.** Histogram of $NO_x$ emissions from diesel passenger cars by emission standard in Switzerland.

fitting distribution, together with its confidence bounds, was then used to characterize the representative emission rate of the corresponding fleet.

- Gumbel Distribution

The Gumbel distribution is appropriate for modeling right-skewed data, such as emission levels influenced by occasional high-emitting vehicles. The probability density function f(x) and cumulative distribution function F(x) of the Gumbel distribution are defined as follows:

$$f(x) = \frac{1}{b} \times e^{-\left(\frac{x-a}{b} + e^{-\frac{x-a}{b}}\right)} \quad (1)$$

$$F(x) = e^{-e^{-\frac{x-a}{b}}} \quad (2)$$

Where $a$ is the location parameter, which equals the mode value and thus and represents the most probable emission rate (the point where the fitted distribution reaches its maximum), and scale parameter $b$ describes the spread of the dataset.

- Laplace Distribution

The Laplace distribution, also known as the double-exponential distribution, is particularly useful for modeling data with sharp peaks and heavier tails than the normal distribution (Kotz et al., 2012). The probability density function f(x) and cumulative density function F(x) of the Laplace distribution are given as follows:

$$f(x) = \frac{1}{2b} \times e^{-\frac{|x-a|}{b}} \quad (3)$$

$$F(x) = \begin{cases} \frac{1}{2} e^{\frac{x-a}{b}}, x < a \\ 1 - \frac{1}{2} e^{-\frac{x-a}{b}}, x \geq a \end{cases} \quad (4)$$

Where $a$ represents the peak or the mean of the distribution, and $b$ is the scale parameter, which controls the spread or variability of the distribution.

### 3.4. Limit of detection determination

In this study, background noise is estimated from ultra low emission electric vehicles (ULEVs), which include BEVs and petrol HEVs. These vehicles are expected to emit no, or negligible $NO_x$ locally, under normal conditions (Knoll et al., 2024). Diesel HEVs and other fuel hybrids were excluded from the analysis. In optical remote sensing measurements, pollutant concentrations are expressed as ratios relative to $CO_2$ (e.g., $NO_x/CO_2$) (Bishop and Stedman, 1996) and can subsequently be converted to fuel-specific emission factors (expressed in grams of pollutant per kilogram of fuel, g/kg) (ICCT, 2018). All ULEV records used for LoD derivation were verified to be based on valid $CO_2$ measurements, ensuring that the data are not affected by near-zero $CO_2$ concentration values, which can occur when the $CO_2$ signal from the exhaust plume is too weak and may artificially inflate the calculated emission factor.

To ensure the noise characterization was not biased by any small, real positive emissions from these vehicles, a mirroring technique was applied. Specifically, only the portion of the ULEV measurement distribution to the left of its mode was used for the analysis, as it is assumed to represent pure instrument noise. This lower half of the distribution was then mirrored to construct a perfectly symmetric dataset. This mirrored dataset was then fitted to a Laplace distribution, providing a complete and interpretable model of the instrument noise characteristics.

Following the approach recommended by Cantwell (2025), the standard deviation of ULEV measurements, serving as low-concentration samples, is calculated and used to estimate the background noise of remote sensing devices.

$$background\ noise = \sigma_{ULEV} \quad (5)$$

Specifically, the LoD is defined as three times the background noise, following the method recommended by the U.S. Environmental Protection Agency (US EPA, 2015; Cantwell, 2025):

$$LoD = 3 * background\ noise \quad (6)$$

Beyond simply estimating background noise, this study also tests whether the $NO_x$ distributions of ULEVs follow a Laplace distribution.

The Laplace distribution, widely used in differential privacy[6] to model controlled noise (Sarathy and Muralidhar, 2011), has also been applied to characterize instrument noise in remote sensing studies (Pokharel et al., 2001). If ULEV $NO_x$ measurements conform to a Laplace distribution, it would further support the use of their distribution's standard deviation as a reliable indicator of background noise.

To investigate whether the low $NO_x$ measurements from Euro 6 diesel vehicles reflect actual emissions or are primarily dominated by instrument noise, a two-sample Anderson-Darling test is conducted to compare the $NO_x$ distributions of ULEVs and Euro 6 series fleets (including Euro 6 ab, 6d-TEMP, and 6d). If the diesel fleets' $NO_x$ measurements also follow a Laplace distribution with a similar location parameter and scale parameter to that of ULEVs, it would suggest that their measurements are largely governed by instrument noise rather than true $NO_x$ emissions.

## 4. Results

### 4.1. Instrument noise and limit of detection

Since the noise distribution is expected to be symmetrical around zero, both Normal and Laplace distributions were fitted to the $NO_x$ emission data from ULEVs in each campaign to identify which model best represents the instrument noise. A goodness-of-fit comparison (Table S. 2) confirmed that the Laplace distribution provided a superior fit for all fleets and was therefore selected to characterize the background noise and calculate the corresponding LoD. The key parameters from the Laplace fits are presented in Table 3. The location parameter represents the instrument's offset, while the scale parameter is used to derive the background noise and LoD. All uncertainties, shown in parentheses, are 95 % confidence intervals generated from 1000 bootstrap replicates.

ULEV data from the Prague and Switzerland-2023 campaigns were excluded due to quality control issues as: in the Prague campaign, although over 300 ULEV measurements were recorded, all license plate recognition entries were marked as false, indicating unreliable data and necessitating exclusion; and in the Switzerland-2023 campaign, while valid data were available, the median $NO_x$ concentration among ULEVs was unusually high at 1.2 g/kg, compared to much lower values observed in other campaigns using the same OPUS device. This suggests that the instrument lacked sufficient sensitivity to reliably detect low-concentration emissions.

**Table 3**
Instrument noise characteristics and detection limits derived from Laplace modeling (g/kg).

| Instrument | Campaign | Location value (95 % CI) | Scale value (95 % CI) | Background noise | LoD |
|---|---|---|---|---|---|
| OPUS | Switzerland-OPUS | 0.11 (0.08, 0.15) | 0.31 (0.29, 0.34) | 0.42 | 1.26 |
| | Krakow | −0.23 (−0.29, −0.14) | 0.89 (0.83, 0.94) | 1.26 | 3.78 |
| HEAT | Switzerland-HEAT | 0.45 (0.34, 0.54) | 0.49 (0.43, 0.55) | 0.69 | 2.07 |
| | Milan | −0.01 (−0.07, −0.05) | 0.26 (0.21, 0.30) | 0.35 | 1.05 |

Among the evaluated instruments, the HEAT device used in Milan recorded the lowest background noise (0.35 g/kg), indicating superior measurement precision and sensitivity (LoD = 1.05 g/kg). Similarly, for campaigns using the OPUS device, the Switzerland-OPUS instrument exhibited lower background noise (0.42 g/kg) and a lower LoD (1.26 g/kg) compared to other OPUS deployments. Negative location values were observed in the Milan campaign and the Switzerland-OPUS campaign, suggesting a systematic negative offset in the instrument's readings.

Notably, substantial variability in background noise was also observed for the same instrument model across different campaigns. As detailed in Table 2, the campaign in Krakow was conducted under very low ambient temperatures (5.7 °C), while the Switzerland campaign was situated on a high-speed motorway with smooth-flowing traffic. It is plausible that these distinct environmental and operational conditions influence the instrument's background noise. However, a more definitive analysis would require a larger ULEV dataset that includes concurrent measurements of environmental variables. Such an analysis would be necessary to distinguish between various potential noise sources (such as physical shaking, electronic interference, or chemical issues (Pokharel et al., 2001)) and ultimately to develop site-specific correction factors. In conclusion, ULEV measurements from all campaigns, except those excluded due to data quality issues, were found to follow a Laplace distribution. Low-concentration $NO_x$ measurements from ULEVs have been validated as suitable inputs for estimating the background noise and detection limit of remote sensing devices. A lower background noise reflects improved measurement stability and enhances the device's ability to detect smaller pollutant concentrations with greater confidence.

### 4.2. $NO_x$ emission trend characterization

By separately applying the Gumbel and Laplace distributions to each subset and selecting the distribution with highest $R^2$ value as the best fit for describing fleet characteristics, the typical emission rates of diesel passenger cars from Euro 4 to Euro 6d are derived. Specifically, all fleets from Euro 4 to Euro 6ab follow the Gumbel distribution.[7] For Euro 6d-TEMP and Euro 6d fleets, the Milan campaign, the Switzerland-HEAT campaign, and the Switzerland-2023 campaign follow the Gumbel distribution while the remaining campaigns follow the Laplace distribution. In conclusion, earlier-generation vehicles are better characterized by the Gumbel distribution, while newer models (Euro 6d-TEMP and Euro 6d) begin to exhibit characteristics of the Laplace distribution in certain cases.

Fig. 5 presents the emission trends of diesel cars across different campaigns. A substantial improvement in $NO_x$ emission performance has been observed for diesel passenger cars since the introduction of Euro 6 ab. Among Euro 4 to Euro 6 ab vehicles, the Switzerland-HEAT campaign recorded the lowest emission rates. This may be attributed to higher highway speeds leading to elevated combustion temperatures (affecting EGR control) and higher SCR temperatures within the effective thermal window (as summarized in Table 2). Similar observations were reported by O'Driscoll et al. (2018) and Yang et al. (2022), suggesting that high engine load does not necessarily result in high $NO_x$ emissions from diesel vehicles.

In contrast, the Switzerland-2023 campaign exhibited the highest $NO_x$ emissions for Euro 4 to Euro 6 ab diesel passenger cars, even

[6] Differential privacy denotes a mathematical approach for preserving the privacy of individual contributions by adding carefully calibrated Laplace noise, ensuring that the output of a query remains almost unchanged whether a single data point is included or excluded.

[7] Detailed information on the measurement count, $R^2$ values of the matching distribution, and the location value for each fleet are summarized in Table S. 3 in the Supplementary materials. The corresponding fitting distributions for each Euro standard in each campaign are summarized in Table S. 4 in the Supplementary materials.

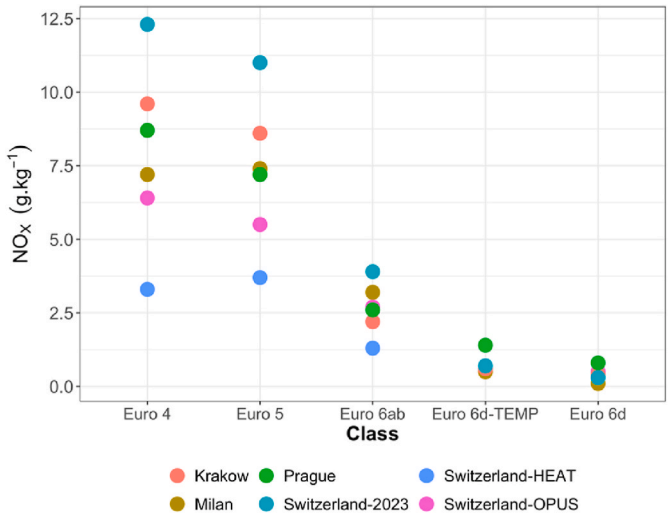


**Fig. 5.** Typical $NO_x$ emissions for diesel passenger cars in different campaigns.

surpassing the Krakow campaign, where extremely low ambient temperatures (as low as 5.7 °C) influence emission rates. Notably, the Switzerland-2023 campaign is the most recent of all campaigns, resulting in the Euro 4 to Euro6ab vehicles involved being relatively older. This suggests that vehicle deterioration may be impacting emission rates. For Euro 6d-TEMP and Euro 6d vehicles, emission rates were consistently low across different campaigns. Specifically, the Milan campaign, which utilized the EDAR HEAT device, recorded a typical $NO_x$ emission rate of only 0.1 g/kg, suggesting that $NO_x$ emissions from Euro 6d-TEMP and Euro 6d diesel vehicles may have approached the detection limit.

### *4.3. Limit of detection significance*

As shown in Section 4.2, the emission distributions for all fleets from Euro 4 to Euro 6 ab were consistently found to follow the Gumbel distribution. However, for the cleaner Euro 6d-TEMP and Euro 6d fleets, a mixed pattern was observed, where some fleets follow a Laplace distribution while others follow a Gumbel distribution. Based on this observation, it was hypothesized that the shape of the measured distribution is indicative of the signal-to-noise ratio. Specifically, it is suspected that if a fleet's emissions are largely below the LoD, its measured distribution will resemble the Laplace distribution, indicating it is noise-dominated. Conversely, if a fleet has significant and right-skewed real emissions, the Gumbel distribution will provide a better fit, suggesting that the true emission signal is dominant.

To validate this hypothesis, a full Laplace distribution was fitted to the data from diesel fleets that also exhibited a Laplace-like shape (i.e., Euro 6d-TEMP and Euro 6d fleets of Switzerland-OPUS campaign and Krakow campaign). The scale parameter for each of these fleets was then compared to the benchmark noise scale parameter, which was previously derived from the ULEV data.

Table 4 illustrate the comparison of Laplace scale parameters for the instrument noise and diesel fleet emission distributions. While the Laplace distribution provided an excellent fit for the Euro 6d-TEMP and Euro 6d of Switzerland-OPUS campaign and Krakow campaign data, the ULEV-derived noise parameter did not fall within the 95 % confidence intervals of the diesel fleets. However, the fitted values were only marginally higher than the noise benchmark. This suggests that these distributions are strongly noise-influenced, with a minor contribution from true vehicle emissions.

**Table 4**
Laplace Scale Parameters for Instrument Noise and Diesel Fleet Emissions in OPUS campaigns.

| Campaign | Scale parameter for instrument noise | Emission standard | Scale value (95 % CI) | Anderson–Darling p-value |
|---|---|---|---|---|
| Switzerland-OPUS | 0.31 | Euro 6d-TEMP | 1.02 (0.88, 1.18) | 0.27 |
| | | Euro 6d | 1.09 (0.72, 1.45) | 0.60 |
| Krakow | 0.89 | Euro 6d-TEMP | 1.23 (1.12, 1.36) | 0.13 |
| | | Euro 6d | 1.34 (1.18, 1.49) | 0.84 |

## 5. Conclusions and outlook

This study evaluated $NO_x$ emission levels of light-duty diesel passenger vehicles across six recent European remote sensing campaigns, with a particular focus on determining whether emissions from the latest Euro 6 series vehicles exceed the detection limit. Results confirm a substantial reduction in $NO_x$ emissions since the introduction of Euro 6 ab standards, with Euro 6d-TEMP and Euro 6d vehicles approaching zero emissions in several campaigns.

To evaluate the instrument's performance under field conditions, a data-driven method was implemented to estimate background noise and the LoD. This approach utilized $NO_x$ measurements from ultra-low-emission reference vehicles (including battery electric and petrol hybrid models), which are assumed to emit negligible $NO_x$. To isolate the symmetrical noise component from any residual positive emission signals, the lower 50th percentile of the reference vehicle data was mirrored to create a perfectly symmetric distribution. This procedure effectively removes the influence of the small, right-skewed tail caused by occasional real-world emissions, allowing for a more accurate characterization of the instrument's inherent background noise. The resulting symmetric dataset was shown to follow a Laplace distribution, confirming its suitability for modeling instrument noise. Based on this noise model, the LoD was estimated. Results revealed that a large proportion of Euro 6d-TEMP and Euro 6d vehicle measurements fell below the estimated LoD. Moreover, in several campaigns employing the filter-based NDUV remote sensing system (OPUS RSD), distribution fitting indicated a shift from signal-dominated to noise-dominated emission behavior in newer Euro 6d-TEMP and Euro 6d vehicles.

The significance of a well-defined LoD is twofold. First, it is crucial for accurately characterizing modern low-emission fleets by distinguishing genuine low-emission measurements from instrument noise, ensuring that the performance of the cleanest vehicles is not misinterpreted. Second, a clear LoD is essential for maintaining the reliability of high-emitter identification. When a substantial proportion of measurements approaches the detection limit, the observed data distribution becomes dominated by instrument noise, which can distort the statistical thresholds used to identify high emitters (Yang et al., 2022; Ghaffarpasand et al., 2023). As a result, the separation between truly clean vehicles and gross polluters becomes less reliable, undermining the primary goal of remote sensing programs. Future research should therefore focus on developing robust statistical approaches to distinguish genuine high emitters under low-emission conditions and on enhancing instrumentation to improve detection sensitivity.

Looking ahead, as the number of electric vehicles especially battery electric vehicles on the road continues to grow, the method developed in this study could enable routine, day-to-day estimation of the LoD in remote sensing campaigns. This would be particularly valuable in the

context of the European Commission (2025) proposed 'Roadworthiness Package', which aims to implement large-scale, routine remote sensing to screen at least 30 % of the vehicle fleet across all EU member states. Given that frequent manual calibration is often impractical, the ability to estimate LoD directly from ULEV measurements would support more effective and adaptive monitoring. This also opens new opportunities for research on how environmental factors such as temperature, humidity, and other ambient conditions, as well as traffic conditions affect instrument detection capabilities in real-world settings, ensuring more robust and reliable remote sensing applications under routine regulatory use.

## CRediT authorship contribution statement

**Zhuoqian Yang:** Writing – original draft, Visualization, Validation, Methodology, Formal analysis, Conceptualization. **Christopher Rushton:** Writing – review & editing, Methodology, Data curation. **James Tate:** Writing – review & editing, Supervision, Funding acquisition, Conceptualization.

## Declaration of competing interest

The authors declare that they have no known competing financial interests or personal relationships that could have appeared to influence the work reported in this paper.

## Acknowledgments

This study has benefited greatly from the use of the Horizon 2020 CARES project (grant agreement no 814966) and ReMOVES database.

Zhuoqian Yang acknowledges the support of the Institute for Transport Studies travel grant to facilitate this research.

## Appendix A. Supplementary data

Supplementary data to this article can be found online at https://doi.org/10.1016/j.jenvman.2025.127767.

## Data availability

The authors do not have permission to share data.

## References

Armbruster, D.A., Pry, T., 2008. Limit of blank, limit of detection and limit of quantitation. Clin. Biochem. Rev. 29 (Suppl. 1), S49–S52.

Bernard, Y., Lee, K., Nepali, R., Tietge, U., Bedogni, M., Wagner, R., Carslaw, D., 2023. CARES deliverable D3.4 – Summary report on partner cities' measurements campaigns. https://cares-project.eu/wp-content/uploads/2023/06/CARES-814966-D3.4-Summary-report-on-partner-cities-measurement-campaigns.pdf [Accessed 25/10/2025].

Betschart, M., Engelmann, D., Comte, P., Bernard, Y., Lee, K., Tietge, U., Mock, P., Borken-Kleefeld, J., Plogmann, J., Eggenschwiler, P., 2022. ReMOVES: Remote Monitoring of Onroad Vehicle Emissions in Switzerland. https://www.aramis.admin.ch/Texte/?ProjectID=45536 [Accessed 25/10/2025].

Bishop, G.A., Schuchmann, B.G., Stedman, D.H., Lawson, D.R., 2012. Multi-species Remote Sensing of Vehicle Emissions on Sherman Way in Van Nuys California. J. Air & Waste Manage. Assoc., 62:10, 1115-1121. DOI: 10.1080/10962247.2012.699015.

Bishop, G.A., Stedman, D.H., 1996. Measuring the emissions of passing cars. Accounts Chem. Res. 29, 489–495.

Bishop, G.A., Stedman, D.H., 2014. On-Road Remote Sensing of Automobile Emissions in the Denver Area: Winter 2013.

Borken-Kleefeld, J., 2013. Guidance Note About on-road Vehicle Emissions Remote Sensing. International Council on Clean Transportation, Vienna.

Borken-Kleefeld, J., Bernard, Y., Carslaw, D., Sjödin, Å., Tate, J., Alt, G.-M., De La Fuente, J., Mcclintock, P., Gentala, R., Hausberger, S., Jerksjö, M., 2018. Contribution of Vehicle Remote Sensing to in-service/real Driving Emissions Monitoring - CONOX Task 3 Report. Swiss Federal Office for the Environment (FOEN).

Borken-Kleefeld, J., Dallmann, T., 2018. Remote sensing of motor vehicle exhaust emissions. International Council on Clean Transportation - White Paper. https://theicct.org/wp-content/uploads/2021/06/Remote-sensing-emissions_ICCT-White-Paper_01022018_vF_rev.pdf [Accessed 24/10/2025].

Cantwell, H., 2025. Eurachem Guide: The Fitness for Purpose of Analytical Methods – A Laboratory Guide to Method Validation and Related Topics (3rd ed. 2025). Available from http://www.eurachem.org.

Carslaw, D.C., Beevers, S.D., Tate, J.E., Westmoreland, E.J., Williams, M.L., 2011. Recent evidence concerning higher NOx emissions from passenger cars and light duty vehicles. Atmos. Environ. 45, 7053–7063.

Carslaw, D.C., Rhys-Tyler, G., 2013. New insights from comprehensive on-road measurements of NOx, NO2 and NH3 from vehicle emission remote sensing in London, UK. Atmos. Environ. 81, 339–347.

Chen, Y., Borken-Kleefeld, J., 2014. Real-driving emissions from cars and light commercial vehicles – results from 13 years remote sensing at Zurich/CH. Atmos. Environ. 88, 157–164.

Chen, Y., Sun, R., Borken-Kleefeld, J., 2020. On-Road NOx and smoke emissions of diesel light commercial vehicles–combining remote sensing measurements from across Europe. Environ. Sci. Technol. 54, 11744–11752.

Chen, Y., Zhang, Y., Borken-Kleefeld, J., 2019. When is enough? Minimum sample sizes for On-Road measurements of car emissions. Environ. Sci. Technol. 53, 13284–13292.

Crowther, J.B., 2001. 12 - validation of pharmaceutical test methods. In: AHUJA, S., SCYPINSKI, S. (Eds.), Separation Science and Technology. Academic Press.

Davison, J., Bernard, Y., Borken-Kleefeld, J., Farren, N.J., Hausberger, S., Sjödin, Å., Tate, J.E., Vaughan, A.R., Carslaw, D., 2020. Distance-based emission factors from vehicle emission remote sensing measurements. Sci. Total Environ. 739, 139688.

De Ruiter, J., Kadijk, G., Elstgeest, M., Ligterink, N.E., Van Der Mark, P.J., 2020. Emissions of Five Euro 6d-Temp Light Duty Diesel Vehicles. TNO.

EUROPEAN COMMISSION, 2025. Proposal for a Directive of the European Parliament and of the Council Amending Directive 2014/45/EU on Periodic Roadworthiness Tests for Motor Vehicles and Their Trailers and Directive 2014/47/EU on the Technical Roadside Inspection of the Roadworthiness of Commercial Vehicles Circulating in the Union.

Gallus, J., Kirchner, U., Vogt, R., Benter, T., 2017. Impact of driving style and road grade on gaseous exhaust emissions of passenger vehicles measured by a portable emission measurement system (PEMS). Transport. Res. Transport Environ. 52, 215–226.

García-Contreras, R., Soriano, J.A., Fernández-Yáñez, P., Sánchez-Rodríguez, L., Mata, C., Gómez, A., Armas, O., Cárdenas, M.D., 2021. Impact of regulated pollutant emissions of euro 6d-Temp light-duty diesel vehicles under real driving conditions. J. Clean. Prod. 286, 124927.

Ghaffarpasand, O., Ropkins, K., Beddows, D.C.S., Pope, F.D., 2023. Detecting high emitting vehicle subsets using emission remote sensing systems. Sci. Total Environ. 858, 159814.

Grange, S.K., Farren, N.J., Vaughan, A.R., Rose, R.A., Carslaw, D.C., 2019. Strong temperature dependence for light-duty diesel vehicle NOx emissions. Environ. Sci. Technol. 53, 6587–6596.

Gruening, C., Bonnel, P., Clairotte, M., Giechaskiel, B., Valverde, V., Zardini, A., Carriero, M., 2019. Potential of Remote Sensing Devices (RSDs) to screen vehicle emissions. EUR 29871 EN, Publications Office of the European Union, Luxembourg, 2019, ISBN 978-92-76-11820-6, doi:10.2760/277092, JRC117894.

Huang, Y., Organ, B., Zhou, J.L., Surawski, N.C., Hong, G., Chan, E.F.C., Yam, Y.S., 2018. Remote sensing of on-road vehicle emissions: mechanism, applications and a case study from Hong Kong. Atmos. Environ. 182, 58–74.

Huang, Y., Organ, B., Zhou, J.L., Surawski, N.C., Yam, Y.-S., Chan, E.F.C., 2019. Characterisation of diesel vehicle emissions and determination of remote sensing cutpoints for diesel high-emitters. Environ. Pollut. 252, 31–38.

ICCT, 2018. Determination of real-world emissions from passenger vehicles using remote sensing data. The International Council on Clean Transportation https://theicct.org/wp-content/uploads/2021/06/TRUE_Remote_sensing_data_20180606.pdf [Accessed 25/10/2025].

Jiménez-Palacios, J.L., 1999. Understanding and Quantifying Motor Vehicle Emissions with Vehicle Specific Power and TILDAS Remote Sensing. Thesis, Massachusetts Institute of Technology.

Knoll, M., Penz, M., Schmidt, C., Pöhler, D., Rossi, T., Casadei, S., Bernard, Y., Hallquist, Å.M., Sjödin, Å., Bergmann, A., 2024. Evaluation of the point sampling method and inter-comparison of remote emission sensing systems for screening real-world car emissions. Sci. Total Environ. 932, 171710.

Kotz, S., Kozubowski, T., Podgorski, K., 2012. The Laplace Distribution and Generalizations: a Revisit with Applications to Communications, Economics, Engineering, and Finance. Springer Science & Business Media.

Mahesh, S., Mcnabola, A., Smith, W., Timoney, D., Ekhtiari, A., Fowler, B., Willis, P., Rose, R., Wareham, J., Walker, H., Ghosh, B., 2023. On-road remote sensing of vehicles in Dublin: measurement and emission factor estimation. Transport. Res. Transport Environ. 117, 103620.

Mulholland, E., Miller, J., Bernard, Y., Lee, K., Rodríguez, F., 2022. The role of NOx emission reductions in euro 7/VII vehicle emission standards to reduce adverse health impacts in the EU27 through 2050. Transport Eng. 9, 100133.

O'Driscoll, R., Stettler, M.E.J., Molden, N., Oxley, T., Apsimon, H.M., 2018. Real world CO2 and NOx emissions from 149 euro 5 and 6 diesel, gasoline and hybrid passenger cars. Sci. Total Environ. 621, 282–290.

Pokharel, S.S., Bishop, G.A., Stedman, D.H., 2001. On-road remote sensing of automobile emissions in the Phoenix area: Year 2; Coordinating Research Council, Inc: Alpharetta, 2001.

Ropkins, K., Defries, T.H., Pope, F., Green, D.C., Kemper, J., Kishan, S., Fuller, G.W., Li, H., Sidebottom, J., Crilley, L.R., Kramer, L., Bloss, W.J., Stewart Hager, J., 2017. Evaluation of EDAR vehicle emissions remote sensing technology. Sci. Total Environ. 609, 1464–1474.

Rushton, C.E., Tate, J.E., Shepherd, S.P., 2021. A novel method for comparing passenger car fleets and identifying high-chance gross emitting vehicles using kerbside remote sensing data. Sci. Total Environ. 750, 142088.
Rushton, C.E., Tate, J.E., Shepherd, S.P., Carslaw, D.C., 2018. Interinstrument comparison of remote-sensing devices and a new method for calculating on-road nitrogen oxides emissions and validation of vehicle-specific power. J. Air Waste Manag. Assoc. 68, 111–122.
Rushton, C.E., Tate, J.E., Sjödin, Å., 2025. A modern, flexible cloud-based database and computing service for real-time analysis of vehicle emissions data. Urban Informatics 4, 1.
Sarathy, R., Muralidhar, K., 2011. Evaluating laplace noise addition to satisfy differential privacy for numeric data. Trans. Data Priv. 4, 1–17.
Smit, R., Awadallah, M., Bagheri, S., Surawski, N.C., 2022. Real-world emission factors for SUVs using on-board emission testing and geo-computation. Transport. Res. Transport Environ. 107, 103286.
Smit, R., Ayala, A., Kadijk, G., Buekenhoudt, P., 2025. Excess pollution from vehicles—A review and outlook on emission controls, testing, malfunctions, tampering, and cheating. Sustainability 17, 5362.
Smit, R., Bainbridge, S., Kennedy, D., Kingston, P., 2021. A decade of measuring on-road vehicle emissions with remote sensing in Australia. Atmos. Environ. 252, 118317.
Söderena, P., Laurikko, J., Weber, C., Tilli, A., Kuikka, K., Kousa, A., Väkevä, O., Venho, A., Haaparanta, S., Nuottimäki, J., 2020. Monitoring euro 6 diesel passenger cars NOx emissions for one year in various ambient conditions with PEMS and NOx sensors. Sci. Total Environ. 746, 140971.
Suarez-Bertoa, R., Valverde, V., Clairotte, M., Pavlovic, J., Giechaskiel, B., Franco, V., Kregar, Z., Astorga, C., 2019. On-road emissions of passenger cars beyond the boundary conditions of the real-driving emissions test. Environ. Res. 176, 108572.
US EPA, 2015. Guidelines establishing test procedures for the analysis of pollutants (Appendix B to Part 136). https://www.ecfr.gov/current/title-40/chapter-I/subchapter-D/part-136 [Accessed 25/10/2025].
Weitkamp, C., 2005. Range-Resolved Optical Remote Sensing of the Atmosphere, vol.102. Springer-Verlag, New York, pp. 241–303.
Yang, Z., Han, K., Liao, L., Wu, J., 2024. Using multi-source data to identify high NOx emitting heavy-duty diesel vehicles. Transport. Res. Transport Environ. 134, 104332.
Yang, Z., Tate, J.E., Rushton, C.E., Morganti, E., Shepherd, S.P., 2022. Detecting candidate high NOx emitting light commercial vehicles using vehicle emission remote sensing. Sci. Total Environ. 823, 153699.